

## **The Design of a Ferrofluid Magnetic Pipette**

Nancy Greivell  
Center for Bioengineering  
University of Washington  
Seattle, WA 98195

Blake Hannaford, Ph.D. \*  
Department of Electrical Engineering  
University of Washington  
Seattle, WA 98195-2500

\* Corresponding author

## **Abstract**

An electromagnetic pipette using a ferrofluid was designed to sample liquid volumes smaller than 0.2 microliter. Submicroliter sample sizes are desirable for reducing the amount of costly reagents and reducing sample requirement for large-scale analysis. The pipette consists of four electromagnets arranged such that air-gaps are aligned to accommodate a tube. A light-hydrocarbon-based ferrofluid is contained in the tube and acts as a plunger. The position of the ferrofluid in the tube was controlled to within 0.2 mm by combining adjacent air-gap magnetic fields. The position of the ferrofluid as a function of time and magnetic pressure as a function of position was measured in one electromagnet air-gap from the device. Maximum pressure measured was 770 Pascals which corresponds to a maximum velocity of 0.9 cm/s. The assembled pipette weighs approximately 25 grams and it measures 4 cm long, 1 cm wide, and 3 cm high.

**Key words:** ferrofluids, ferrofluidics, electromechanical device, electromagnetic device, electromagnetic pipette, ferrofluid flow, sample handling.

## 1. Introduction

The handling of biological liquids for chemical analysis is a time-consuming and tedious job in biochemical laboratories. Much of the liquid handling is done on automated instruments by a device consisting of a plunger in a bore operated by a mechanical linear actuator. The discrete movement of the plunger by the linear actuator samples a discrete volume of reagents and/or biological fluid. These conventional pipettes can sample an aliquot of liquid as small as 0.2 to 0.5 microliters with about 3-5% degree of precision. Smaller precision pipetting is problematic with these types of mechanical pipettes.

New technological demands in biochemical laboratories have motivated the search for methods of handling volumes of liquid smaller than 0.2 microliters. This is particularly true in the research of the human genome and of proteins expressed by the human genome where biochemists are working to automate current methods for large-scale analysis. Minimizing reagent and sample requirements for such large-scale analysis would help reduce the cost of analysis. The ferrofluid-magnetic pipette was designed to address the problem of handling submicroliter liquid volumes smaller than 0.2 microliter. This pipette uses the properties of ferrofluids and the principles of magnetism to sample such quantities of liquid.

Ferrofluids are stable colloidal suspensions of magnetite in a liquid medium [1-3]. Suspending magnetite in a liquid imparts unusual properties to the liquid. Forces are developed in ferrofluids in the presence of a magnetic field. Because of this property, ferrofluids have found their way into a variety of applications such as rotating shaft seals, sensors, and drug delivery in humans [4].

The idea of the ferrofluid-magnetic pipette is similar to a pumping device proposed by C.W. Miller [5]. Miller's proposed pump uses a series of electromagnets to generate a gradient magnetic field which moves the ferrofluid through a length of a tube. This idea was proposed but not actually built. In the ferrofluid-magnetic pipette, a discrete volume of ferrofluid is placed in a small tube and acts as a plunger similar to the spring-loaded plunger in conventional pipettes. To sample a small amount of fluid, the array of electromagnets is used to actuate a position change of the ferrofluid. The resolution of ferrofluid positioning and the inner diameter of the tubing determines the volume of liquid sampled by the device.

This paper presents the theory, design, and testing of the ferrofluid-magnetic pipette device. An analysis of experimental data of the ferrofluid in a gradient magnetic field is discussed. The goal of the project was to develop a reasonable electromagnet configuration and a method of controlling

the position of the ferrofluid with a high resolution.

## 2. Theoretical Calculations

The analysis of the ferrofluid motion in a gradient magnetic field was important for designing the pipette, evaluating its performance, and developing a method of high-resolution position control. This analysis involved computing the velocity of the ferrofluid from pressure measurements to numerically describe the action of the pipette. This section presents the equations used to compute this velocity.

The velocity depends on the type of ferrofluid used in the pipette and its properties. Table 1 summarizes the properties of EMG 901 ferrofluid - a suspension of magnetite in a light hydrocarbon based oil purchased from Ferrofluidics Corporation. It was used in the pipette design and used in pressure and position measurements.

To analyze the ferrofluid in the gradient magnetic field, assumptions are made to simplify the computations. The ferrofluid is assumed to be viscous and incompressible; as long as the windings are sufficiently cooled, fluid flow is also considered to be isothermal [1].  $M$  and  $H$  were assumed to be colinear [3]; the gravity component was assumed negligible in the direction of ferrofluid motion.

The modified ferrohydrodynamic Bernoulli equation [1, 6] is expressed in terms of fluid velocity and simplified to the Hagen-Poiseuille equation to compute ferrofluid velocity for the pipette configuration. The well-known Hagen-Poiseuille equation for flow in a tube of circular cross-section is

$$v = \frac{\Delta p \pi r^2}{8\eta L} \quad (1)$$

where  $\Delta p$  is the pressure drop across the fluid,  $\eta$  is the viscosity,  $r$  is the inner radius of the tube,  $L$  is the length of the ferrofluid in motion [7, 8]. For average fluid velocity in a small diameter tubing under varying pressure, such as the ferrofluid in a gradient-field, a quasi-steady Poiseuille flow was computed with the above equation [7].  $\Delta p$  in equation (1) is

$$\Delta p = \mu \int_{H1}^{H2} M dH \quad (2)$$

where  $M$  is the magnetization of the ferrofluid,  $H$  is the magnetic field, and  $\mu$  is permeability.

Equation (1) assumes the ferrofluid flow in the pipette tubing to be laminar with a constant pressure drop across the length of the tube. Laminar flow was verified by computing the Reynolds number for a smooth walled tubing of inner diameter of less than or equal to 2 mm. The resulting Reynolds number was less than 5 using the density and viscosity from Table 1 and a velocity of 1 cm/s. This velocity was estimated from observing the ferrofluid motion. The magnitude of the Reynolds number that delimits laminar from turbulent flow is approximately 2000 [8].

Equation (2) is just the area under the ferrofluid magnetization curve. A direct application of this equation with an appropriate demagnetization factor results in higher pressures than measured pressures [5, 9]. Therefore, pressure was not computed to predict the ferrofluid motion; instead, we relied on experimental data with equation (2) to qualitatively understand the ferrofluid response to an electromagnet configuration.

### 3. Experiments

There were two sets of data collected which were critical for the pipette design: Magnetic pressure as a function of ferrofluid position in one electromagnet air-gap; and ferrofluid position as a function of time. Measured pressure was used to predict ferrofluid velocity in the gradient magnetic field and to guide the electromagnet placement and the driving current. Measured position was important for evaluating the pipette performance and for controlling ferrofluid position.

The magnetic pressure was measured using the set-up shown in Figure 1. This set-up included one electromagnet from the pipette device and the Tefzel® tubing containing a 22 mm long plug of ferrofluid. Current in the windings was controlled such that the applied mmF was  $96 \pm 5$  amp-turns (A-T). At the start of the pressure measurements, the ferrofluid moved to its equilibrium position with the port open. This equilibrium position marked the point at which  $\Delta p$  was zero. Then, pressure inside the tubing between the ferrofluid and the manometer was increased by injecting air into the port. The position of the ferrofluid plug end with respect to the center of the airgap was recorded with increments of  $\Delta p$  until the magnetic force could no longer hold the ferrofluid in the air-gap of the core. *(insert Fig 1)*

The position of the ferrofluid plug end with respect to the center of the airgap as a function of time was obtained from a video tape of the ferrofluid in motion. To record the ferrofluid motion on VHS, the set-up shown in Figure 1 was placed under a dissecting microscope with a millimeter ruler included for proper scaling. A CCD camera was attached to the microscope and current was

applied to the windings. The motion of the ferrofluid was captured on VHS tape. This recording was digitized at 10 frames per second. Each frame was examined and the position of the ferrofluid was measured to within  $0.1 \pm 0.05$  mm.

A similar set-up was used to measure the resolution of position control of the pipette device. Two cores from the pipette device were held in place under the dissecting scope such that the spacing between the two core gaps was 0.5 mm. The field polarities were opposite with respect to one another. The position change of the ferrofluid was recorded with the camera mounted on the dissecting scope.

## 4. Results and Discussion

This section presents the pipette prototype, the pressure data which guided the design, and the position and velocity data which characterized the ferrofluid and evaluated the performance of the pipette. In addition, the method of controlling the ferrofluid position is discussed.

### *Prototype Design*

The ferrofluid-magnetic pipette consists of 4 iron-toroid cores of rectangular cross-section each wound with 160 turns of 30 AWG wire. The Delrin® casing holds the iron-toroid cores and the Tefzel® tube contains the ferrofluid. The pipette assembly and its parts are shown in Figure 2. The Tefzel® tube containing the ferrofluid is not shown. The toroid cores are arranged in an alternating pattern to accommodate bulk of the windings. *(insert Fig. 2)*

The toroid cores were machined of cast iron which have a high permeability and low coercive field [10]. The dimensions of the iron-cores are: inner diameter of 3.5 mm, outer diameter of 6.5 mm, width of 2.5 mm, and air-gap length of 1.8 mm. Each toroid core and winding generates a gradient magnetic field in the 1.8 mm air-gap.

Tefzel® tubing was chosen for its minimal wetting characteristic with the ferrofluid. The tube inner diameter is 0.4 mm and the outer diameter is 1.6 mm. EMG 901 ferrofluid was chosen because of its high magnetic saturation.

The Delrin® casing consists of 4 pieces (two end pieces and two center pieces) which hold the toroid cores in the configuration shown in Figure 2. Delrin® was chosen because of its “nonmagnetic” property and because it is easy to machine. One end piece of the casing is larger to provide a means of attaching a holder for one end of the Tefzel® tubing. Both end pieces of the casing have a 1.7 mm diameter hole to accommodate the Tefzel® tubing and a hole for inserting a bolt to attach

the pipette to a robotic arm or sampling system. The center pieces are identical such that additional electromagnets can be easily added to the pipette.

The parts of the pipette are easily assembled and held together with two 2-56 by 1 inch bolts. Paper or plastic spacers of ~0.5 mm thick must be placed between the iron cores to prevent the cores from shorting out the magnetic field of its neighboring core. The plastic casing hold the cores such that the air-gaps are aligned and the tubing is securely held inside the air-gap of each toroid core. To prepare the pipette for liquid sampling, a volume of ferrofluid is placed in the Tefzel® tubing by capillary action and the tubing is threaded through the hole provided on the end pieces of the Delrin® casing. The entire assembled pipette weighs approximately 25 grams.

The ends of the windings on the toroid-cores are connected to a current source which supplies  $0.6 \pm 0.03$  amps. This current level will produce an mmF of  $96 \pm 5$  A-T in the 160 turns of wire. The current source can be driven by digital logic such that a logic '1' will provide 0.6 amps and a logic 0 will provide negligible current. The actual current output of this circuit was 0.58 amps for a logic '1' and 0.02 amps for a logic '0'. At 0.6 amps, winding and iron-core temperatures rise to about 130 and 140°F respectively in 15 minutes. Extra cooling should be provided for currents over 0.7 amps.

### ***Magnetic Pressure***

Magnetic pressure on the ferrofluid in the pipette device was measured as described previously. The distance between the high pressure end of the ferrofluid and the center of the air-gap was plotted against the corresponding manometer reading,  $\Delta p$ . Three separate pressure measurements (*insert Fig. 3*) were taken for each position. The average of measured pressures for each position are plotted in Figure 3. The error bars indicate the highest and lowest pressures measured at each position and the center of the air-gap is the 0-mm mark on the position axis.

In Figure 3, the portion of the curve with the highest slope is the region from the edge of the core to 1.5 mm. This is the region where there is maximum mechanical stiffness of ferrofluid plug movement. Based on this observation, the toroid cores were placed to within 0.5 mm of each other to move the ferrofluid in the pipette device. The maximum magnetic pressure at 96 A-T is about 770 Pascals which is near the center of the air-gap; pressures dropped off in the regions of magnetic fringing. The equilibrium position of the ferrofluid, at  $\Delta p = 0$ , was 4.5 mm from the center of the gap.

### ***Position and Velocity***

The position data from the digitized VHS recording of the ferrofluid in one air-gap was plotted *(insert Fig. 4)* as a function of time and shown in Figure 4-A. The center of the air-gap is marked by 0 on the y-axis. The average velocity,  $\Delta z/\Delta t$ , was computed for each time-interval from the position data and plotted as a function of time. This plot is shown in Figure 4-B.

The position curve in Figure 4-A is sigmoid in shape and reflects the slow movement of the ferrofluid in the weaker fringes of the magnetic field with a rapid movement in the center of the air-gap where the magnetic field is stronger. The curve in Figure 4-B shows a sharp increase in velocity where the ferrofluid end is near the center of the air-gap with a decrease in velocity in the regions of magnetic field fringing.

Next, the velocity was plotted as a function of position with respect to the center of the air-gap. Two sets of data were used to compute this velocity. The first set of data was the measured position with respect to time. The second set of data was the experimental static pressure. Figure 5 depicts *(insert Fig. 5)* the velocity computed from the position data (solid line) and the velocity computed from the static pressure data (dashed line). The static pressure was converted to velocity using the Hagen-Poiseuille equation discussed previously. Because the viscosity of the ferrofluid increases with applied magnetic field, a multiple factor of 1.45 was used to correct the ferrofluid viscosity in computing velocity from measured pressure. This factor was obtained from the work by Mozgvoi and McTague [11, 12].

Overall, the position and computed velocity curves match qualitative observations of the ferrofluid motion through the air-gap. The total time for the ferrofluid to move the 6.5 mm distance shown in Figure 4 was roughly 5.5 seconds. The stroke distance of 6.5 mm corresponds to approximately 0.8 microliters. The electromechanical stroke-time for one electromagnet is about 0.5 second. This stroke-time was computed assuming that each toroid-core air-gap is spaced 3 mm apart (center-to-center distance) and it was computed assuming that the next electromagnet was “energized” when the ferrofluid end reaches the center of the 0.5 mm space separating the two adjacent air-gaps. The average velocity of the ferrofluid was about 0.6 cm/s for the electromechanical stroke. To move the ferrofluid by sequentially “energizing” the electromagnets as in Miller’s pumping idea, a circuit must be built to apply current to each current source at a frequency no faster than 2 Hertz.

### ***Position Control***

The pipette prototype was designed to handle submicroliter, or nanoliter, sizes of liquids. To handle liquid volumes in this range, ferrofluid position change must be a few tenths of a millimeter. There were two methods of operating the ferrofluid-magnetic pipette to achieve this resolution.

The first method involved sequentially energizing the electromagnets at about 2 Hertz, called the “sequential-pulsing scheme.” Each electromagnet was “energized” in a specific sequence such that a travelling “wave” of magnetic field was created down the length of the tube at a speed which can be followed by the ferrofluid. The volume sampled by the pipette is expressed as

$$Vol = [NW + (N - 1)S + 2F_d - F_L] \left[ \frac{\pi}{4} (ID)^2 \right] \quad (3)$$

for  $F_L > 2F_d + W$ ; where  $N$  is the number of electromagnets in the pipette,  $W$  is the length of the air-gap along the axis ferrofluid motion in the air-gap (z-axis),  $S$  is the spacing between each electromagnet,  $F_d$  is the length of the fringing field along the z axis on the ends of the electromagnet array,  $F_L$  is the length of the ferrofluid, and  $ID$  is the tubing inner diameter.

The length of the ferrofluid,  $F_L$ , cannot exceed the entire length of the electromagnet array and fringing field on the ends ( $NW + (N - 1)S + 2F_d$ ) otherwise, there would be no magnetic pressure on the ferrofluid when it is centered on the electromagnet array. In addition,  $F_L$  cannot be smaller than  $W$  because the ferrofluid must be pulled through one air-gap such that the field generated by a neighboring electromagnet can act on the ferrofluid with sufficient pressure. For  $W < F_L < (2F_d + W)$ , the ferrofluid will center itself according to the symmetry of the gradient-field in the air-gap.

The “sequential-pulsing scheme” works provided the remnant flux in the core of the energized electromagnet is eliminated prior to removing the current and energizing the next electromagnet. The accuracy of the desired volume handled depended on the accuracy of predicting  $F_L$ ,  $ID$ ,  $F_d$ ,  $W$ , and  $S$ . There was also some concern with the compliance of position control particularly when the ferrofluid reached the ends of the electromagnet array.

The second method of controlling the ferrofluid position involved changing the gradient magnetic field along the axis of ferrofluid motion (z axis). Two adjacent electromagnets were arranged such that the fields generated were opposite in polarity with respect to one another. When both were switched on, the gradient field profile was altered due to the subtraction of the x-component

of magnetic field particularly in the region between the two adjacent air-gaps. This subtraction altered the gradient field and thus altered the resulting magnetic pressure on the ferrofluid plug. *(insert Fig. 6)*

To illustrate the gradient magnetic field alteration, the magnitude of the x-component of the magnetic field of two electromagnets was computed using the circular-arc straight-line model [10, 13] and plotted as a function of position in Figure 6. The resulting computation predicts that the ferrofluid will stop in the region between the two air-gaps when  $\Delta p$  of equation (2) is zero, assuming both ends of the ferrofluid plug are open to atmospheric pressure. Once the ferrofluid comes to rest at  $\Delta p = 0$ , a decrease in the opposing magnetic field of core 2 will cause the ferrofluid to adjust its position due to the change in gradient field distribution. Figure 7 illustrates the general idea of this position control scheme. *(insert Fig. 7)*

To obtain an experimental dynamic analysis of the two-electromagnet arrangement, position as a function of time was measured from a digitized VHS recording of the ferrofluid in the two-electromagnet arrangement. This data is shown in Figure 8. As Figure 6 predicts and as shown in Figure 8, the ferrofluid stopped in the region between the two cores with both electromagnets “on” and readjusted its position when core 2 was switched off. *(insert Fig. 8)*

The position adjustment of the ferrofluid was measured experimentally as described previously. The measurements were taken for 5 different current levels in core 2: 0.095 (15 A-T), 0.18 (29 A-T), 0.34 (54 A-T), 0.44 (70 A-T), and 0.58 amps (93 A-T). The stopping position of the ferrofluid (corresponding to C of Figure 7) was noted; the ferrofluid stopped to within 1.7 to 1.9 mm from the center of the air-gap depending on the level of current applied to core 2. The position change of the ferrofluid was measured to within 0.05 mm after removing the current in the windings of core 2. These results are presented in Table 2 with the corresponding current change. The position change was converted to a corresponding volume change and also summarized in Table 2.

The experimental data in Table 2 shows the effect of the field change in core 2 on the position of the ferrofluid. The remnant magnetic field in core 2 was not eliminated and therefore, the measured ferrofluid position change ranged from 0.1 to 0.5 mm. The advantage of this control scheme over the sequential-pulsing method, was the improved stiffness of position control with the stiffest mechanical position control obtained at approximately 0.2 to 0.3 amp current change in the windings of core 2.

The ferrofluid pipette was tested with the “sequential-pulsing scheme” using water as a sample. This device was able to dispense 90 nl of liquid. Because of magnetic hysteresis in the electromag-

net cores, it was difficult to control the ferrofluid position to dispense smaller quantities of water. To remove the remnant magnetic field, a backwards pulse of current should be applied to the electromagnet immediately after the energizing current is removed.

## **5. Conclusion**

This paper presented the design of the ferrofluid-magnetic pipette. The pipette consists of a ferro-fluid contained in Tefzel® tubing and four electromagnets which generate the magnetic field to control the ferrofluid position. The ferrofluid acts as the plunger as in a mechanical pipette and the position change of the ferrofluid corresponds to a volume sampled by the pipette. A position change of 0.1 to 0.5 mm was achieved by modulating the gradient-field in one electromagnet. The simple design and lack of moving parts is an advantage for manufacturing and maintaining the device.

The next step with the pipette design would be to design software implementing the control scheme presented in the paper. In addition, this software could be made to implement a feed-back type control system which would increase the accuracy of the position control. We envision that the final ferrofluid-magnetic pipette will be used in large-scale analysis such as the Human Genome Project.

## **Acknowledgments**

This work was part of a M.S.E.E. thesis by Nancy Greivell submitted to the Center for Bioengineering at University of Washington. The research was supported by a grant from the Washington Technology Center.

## References

- [1] Rosensweig, R.E., *Ferrohydrodynamics*, (New York, 1985).
- [2] Rosensweig, R.E., 1966, *Int. Sci. Tech.*, 55 (1966) 48.
- [3] Barral, J., R. Bonnefille, M. Duret, et M. Kant, *Revue De Physique Appliquee*, 12 (1977) 1711.
- [4] Raj, K., R. Moskowitz, *Journal of Magnetism and Magnetic Materials*, 85 (1990) 233.
- [5] Miller, C.W., NTIS Final Report AD/A-006323, 1973.
- [6] Neuringer, Joseph L. and Ronald E. Rosensweig, *Phys. Fluids*, 7 (1964) 1927.
- [7] White, Frank M., *Viscous Fluid Flow, Second Edition*, (New York, 1991).
- [8] Benedict, Robert P., *Fundamentals of Pipe Flow*, (New York, 1980).
- [9] Miller, C.W., E.L. Resler, Jr., *Phys. Fluids*, 18 (1975) 1112.
- [10] Roters, Herbert C., *Electromagnetic Devices*, (New York, 1941).
- [11] McTague, John P., *The Journal of Chemical Physics*, 51 (1969) 133.
- [12] Mozgovoi, E. N., É. Ya. Blum, and A. O. Tsebers, *Magnetohydrodynamics*, 9 (1973) 52.
- [13] Hanselman, Duane C., *Brushless Permanent-Magnet Motor Design*, (New York, 1994).

**Figure Legends:**

**Figure 1.** Setup for taking magnetic pressure measurements as a function of ferrofluid plug end position with respect to the center of the air-gap. One end of the tube was connected to a water-filled manometer. Air was injected in the port and position of the end of the ferrofluid was measured with respect to the center of the air-gap (indicated by '0' on the axis).

**Figure 2.** The assembly of the ferrofluid pipette. The 160 turns of 30 AWG wire is not shown for clarity. The entire assembly is approximately 4 cm long by 1 cm wide by 3 cm high.

**Figure 3.** Magnetic pressure versus position of the ferrofluid plug end with respect to the center of the air-gap. The center of the air-gap is indicated by '0' on the x-axis. Three pressure measurements were taken at each position point. Error bars indicate the highest and lowest pressure measured. Average of the three measurements are plotted as dots. Total length of the ferrofluid plug in the tubing was 22 mm.

**Figure 4.** A: Experimental position of the ferrofluid plug end with respect to the center of the air-gap versus time. The center of the air-gap is indicated by '0' on the y-axis. B: Average velocity of the ferrofluid versus time computed from A. Total length of the ferrofluid plug in the tubing was approximately 20 mm.

**Figure 5.** Velocity versus position of the ferrofluid plug end with respect to the center of the gap. Dashed line: velocities computed from static pressures and corrected for magnetic induced viscosity. Solid line: velocities computed from position versus time data.

**Figure 6.** Estimated magnitude of the x-component of applied magnetic field in the airgap of two adjacent electromagnets. Computations use the circular-arc straight-line approximation [10, 13]. The field in core gap 1 was "energized" at 96 A-T. The field in core 2 was varied from 8 A-T to

128 A-T. Each plot shows the computed field profile in both air-gaps as a result of the addition of the two fields - core 1 is always energized with 96 A-T and core 2 is energized at different levels for each plot.

**Figure 7.** The idea of the gradient-field modulation scheme for ferrofluid position control. In A, core 1 and core 2 are energized simultaneously. The ferrofluid moves through the air-gap of core 1 in B and stops at a point in the space between the two air-gaps in C. At this point, the end of the ferrofluid-magnetic pipette is placed in the biological liquid. Sampling occurs when the field in core 2 is “switched off” and the ferrofluid readjusts its position in D. This position adjustment corresponds to a specific volume of liquid sampled.

**Figure 8.** Measured dynamics of the gradient-field modulation scheme using two electromagnets. The plot shows the end of the ferrofluid plug with respect to the center of the airgap versus time. Dashed line: ferrofluid motion in the tubing with one electromagnet at 96 A-T. Solid line with circles: ferrofluid motion in the tubing with two cores: core 1 at 96 A-T, and core 2 at 48 A-T - at the point indicated, the ferrofluid moved to a new rest position when the current was switched off in windings on core 2.

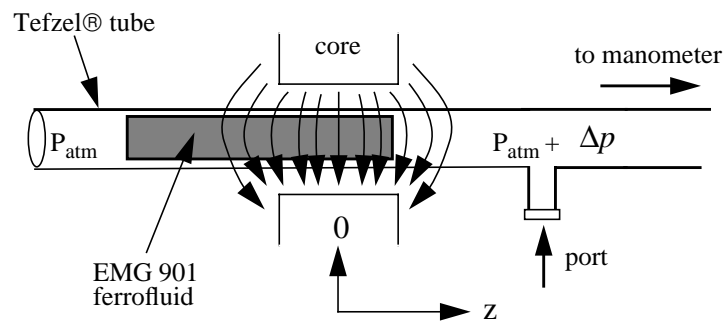
**Table 1: EMG 901 Ferrofluid Physical Properties.\***

Property	value	units
Density @ room temperature	1350	Kg/m <sup>3</sup>
Viscosity @ 27°C	0.143	dyne-sec/cm <sup>2</sup>
Magnetic Saturation	600	Gauss
Particle concentration	10.8	volume%
Particle Size	100	Angstroms = 10 <sup>-10</sup> m

\*These properties were provided by Dr. K. Raj of Ferrofluidics Corporation, Nashua, NH.

**Table 2: Position change and corresponding sample volume.**

current change	position change	corresponding volume
0.58 amps	0.5 mm	63 nl
0.44 amps	0.4 mm	50 nl
0.34 amps	0.3 mm	38 nl
0.18 amps	0.2 mm	25 nl
0.095 amps	0.1 mm	13 nl

*Figure 1*

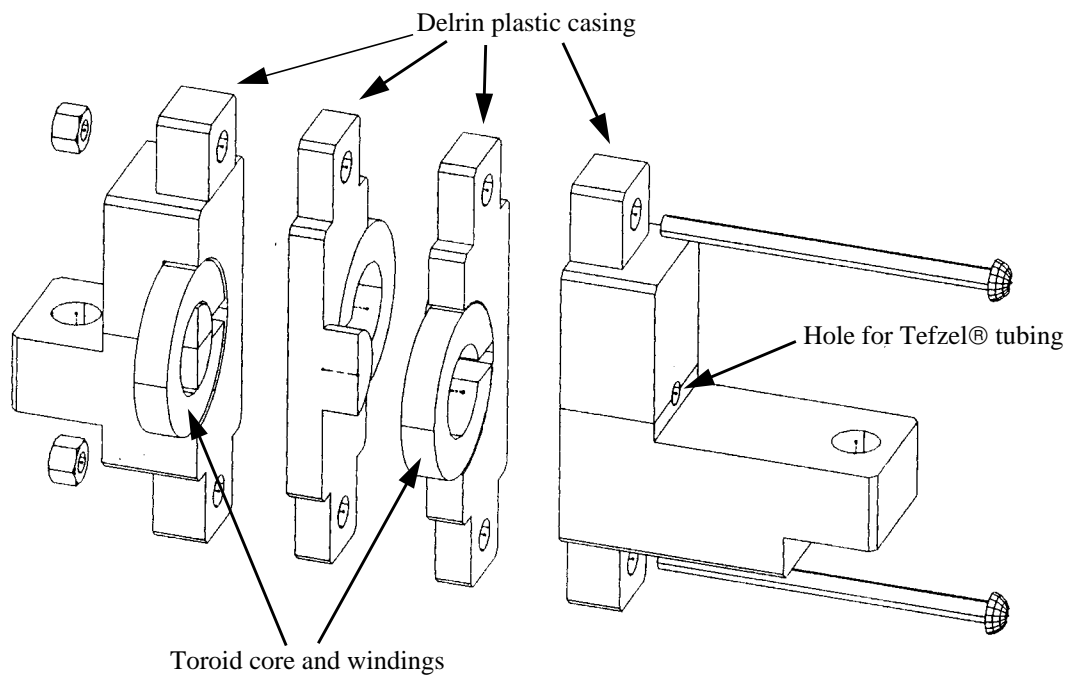
*Figure 2*

Figure 3

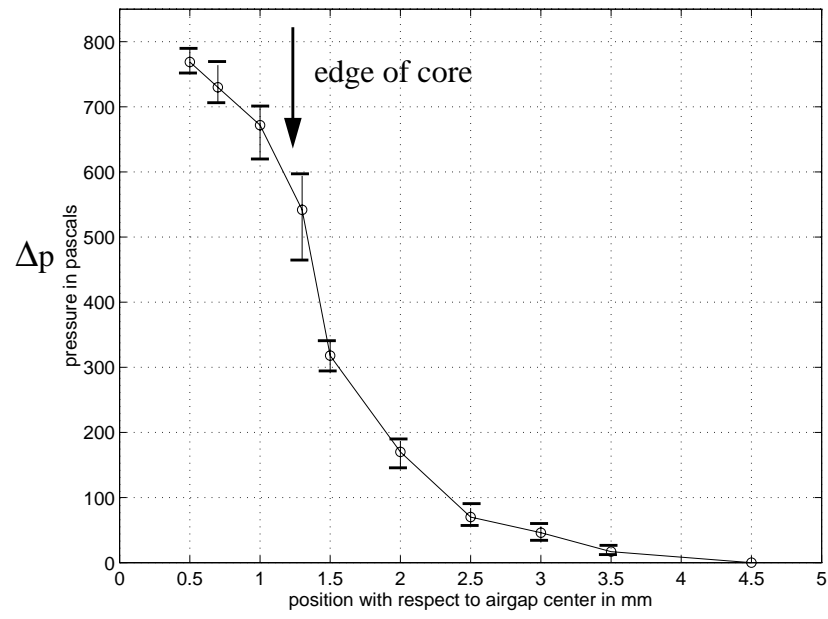


Figure 4

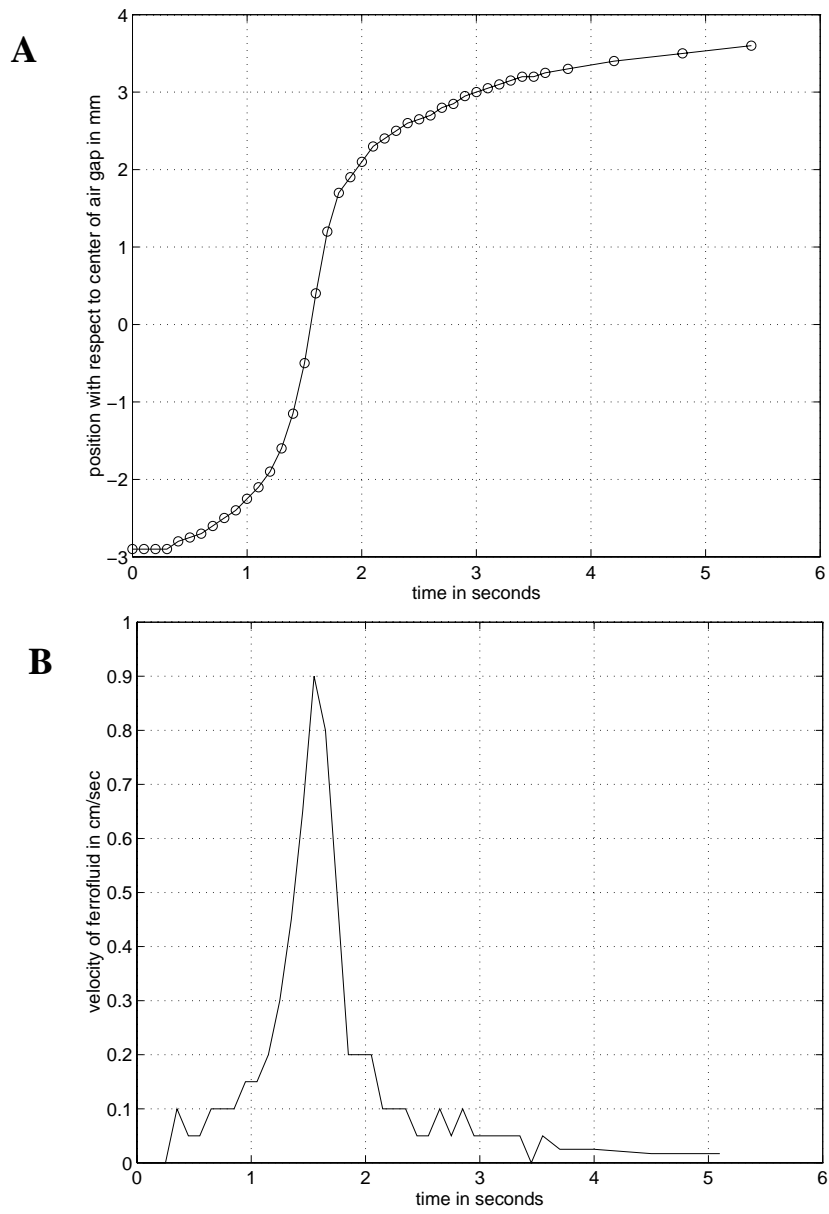


Figure 5

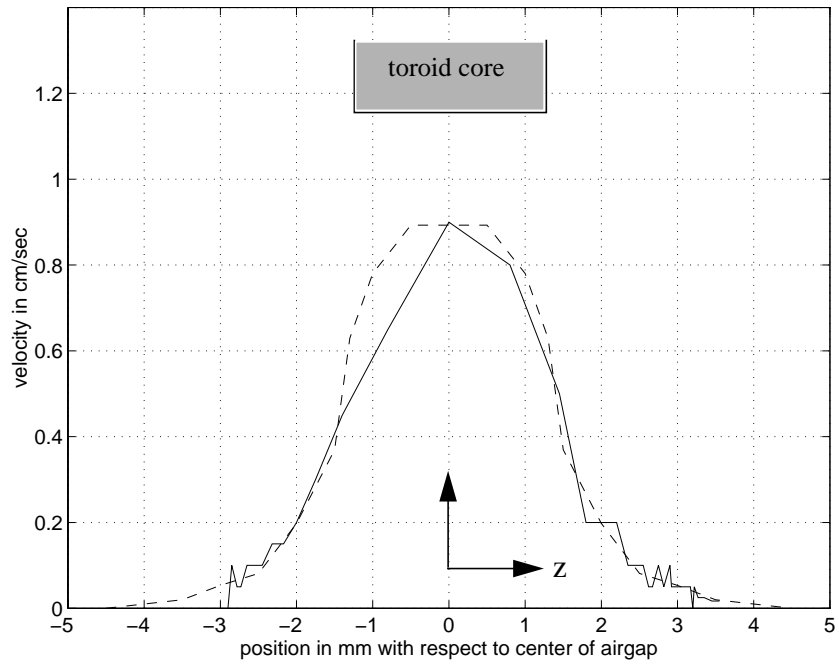




Figure 7

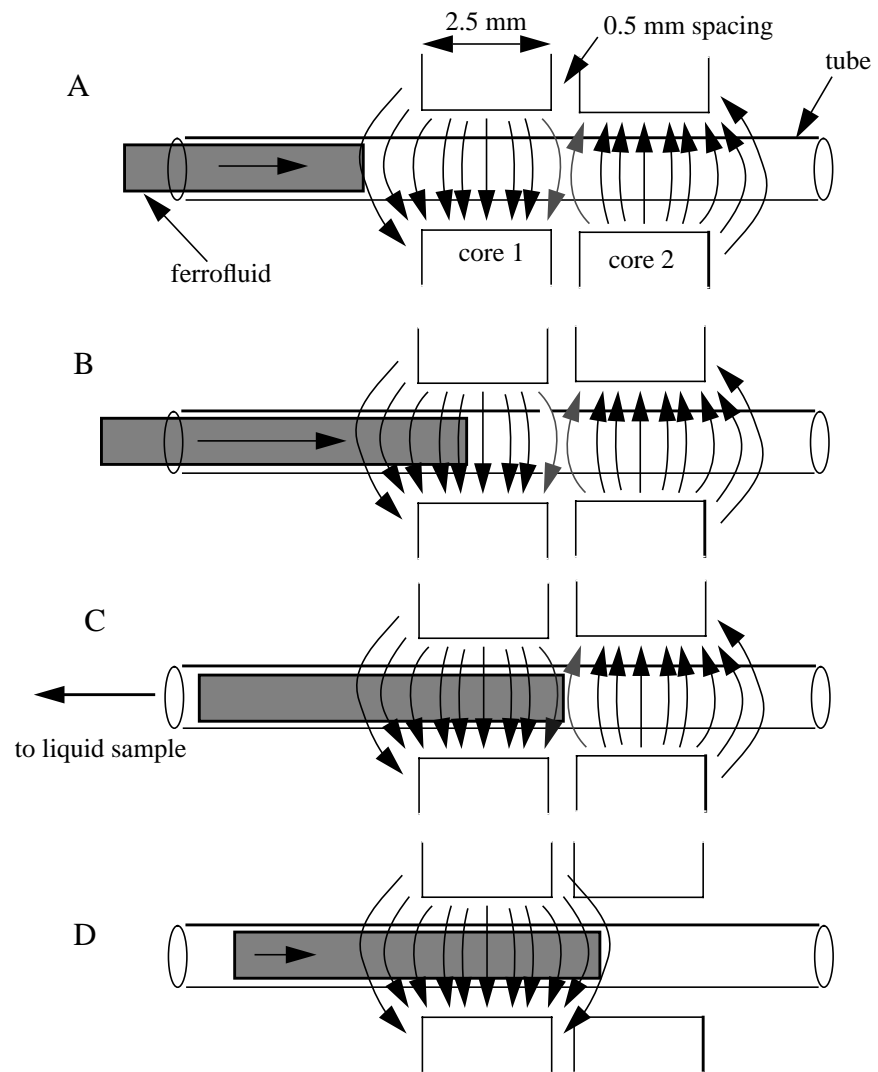


Figure 8

